Progress In Electromagnetics Research, PIER 19, 129–145, 1998

A SEGMENTED APPROACH FOR COMPUTING THE ELECTROMAGNETIC SCATTERING OF LARGE AND DEEP CAVITIES

F. Obelleiro, J. Campos-Niño, J. L. Rodríguez, and A. G. Pino

ETSE Telecomunicación.
Universidade de Vigo.
Campus Universitario s/n.
36200 Vigo. Spain

1. INTRODUCTION

The problem of scattering from large open-ended waveguide cavities has great importance in radar cross section (RCS) prediction of complex targets. This importance is owing to the significant contribution from the interior of jet engine inlets or exhaust ducts to the over-all RCS of real targets like modern aerospace vehicles.

Several approaches have been developed for analyzing large cavities. The first one was modal analysis [1] which still is used as a reference solution to validate other subsequent methods in simple cavities where is possible to find closed-form expressions for waveguide eigenmodes. Some improvements have been proposed in order to increase the ef-

ficiency and accuracy of this method; it is worth mentioning among others [2] and [3].

For arbitrarily shaped cavities, where conventional waveguide modes cannot be defined, the ray and beam techniques [3–5] must be used. However, these methods are restricted to relatively shallow cavities, due to the computational cost and the ray and beam distortion problems associated with deep cavities, in which a high number of internal reflections must be considered. A more efficient approach, the *Generalized Ray Expansion* (GRE) method, was presented in [3, 5, 6]. This approach improves the accuracy of the previous ray-based methods, although it still suffers from ray tracing drawbacks.

In previous papers [7–9], two efficient solutions have been presented, the *Iterative Physical Optics* (IPO) and the *Progressive Physical Optics* (PPO) methods. In these works, the *magnetic field integral equation* (MFIE) is obtained for the equivalent currents in the interior cavity walls, and is solved by using two different algorithms. In the IPO method, the solution is obtained after a number of iterations which is closely related with the number of internal expected reflections; while PPO reaches the solution in a single iteration, by progressive application of *Physical Optics* (PO) according to the wave propagation sense inside the cavity. Thus, PPO is better from the computational point of view, although IPO is applicable to more general shaped cavities [9]. Once the currents are know, the scattered fields can be found using either *aperture integration* (AI) [3] or the *generalized reciprocity integral* (RI) proposed in [10].

In recent works [11–13], some hybrid methods have been presented to analyze cavities containing complex terminations. In all of them, the cavity is divided into two different parts: the front section (typically smooth) which is analyzed by any of the preceding approaches; and the complex termination where more accurate methods, such as the *Method of Moments* (MoM), the *Finite Element Method* (FEM) or the *Finite-Difference Time-Domain* method (FDTD), must be used.

In this paper, we present a sectioning algorithm which extents the scope of application of IPO and PPO methods to very deep cavities. Our solution leads to two different alternatives: namely the segmented version of IPO (S-IPO) and the corresponding of PPO (S-PPO). In both methods, the cavity is subdivided into several sections, and each of them is analyzed independently from the rest of the cavity. The scattering matrices of each section are calculated using either the IPO

or the PPO methods. Finally, a simplified *connection scheme* based on the *Kirchhoff approximation* [10] and the *generalized reciprocity integral* [14] is used to obtain the global response of the whole cavity. Both S-IPO and S-PPO methods provide a considerable reduction of the computational cost with respect to the direct solution while maintaining a good grade of accuracy.

2. FORMULATION

2.1 The Original Problem

First, consider the problem depicted in Fig. 1a, in which an open-ended cavity is illuminated by an incident plane-wave. Although the incident field illuminates both interior and exterior cavity walls, we are only concerned with the interior problem, without considering the scattering due to external cavity surfaces. The cavity walls are considered to be made of perfect electric conductor (PEC) and the surrounding medium is characterized as free space. In the next sections, an $e^{j\omega t}$ time dependence is assumed and suppressed for the field expressions, k refers to the wave-number, and η_0 is the intrinsic impedance of the free space.

2.2 The Equivalent Problem

In order to evaluate the scattered fields from the interior of the cavity, the original problem of Fig. 1a is replaced by the equivalent problem depicted in Fig. 1b [7–9] based on surface equivalent principles [15]. In this equivalent problem, the cavity walls and the plane wave excitation are replaced by electric surface currents $\mathbf{J}_w$ over the cavity walls S_w, and electric and magnetic surface currents $\{\mathbf{J_a}, \mathbf{M}_a\}$ over the aperture S_a. These currents radiate in free space and reproduce exactly the fields $\{\mathbf{E}, \mathbf{H}\}$ within the cavity (volume enclosed by surfaces S_a and S_w). The coupling between the excitation plane wave and the cavity is performed through the surface currents $\{\mathbf{J}_a, \mathbf{M}_a\}$ in the aperture S_a. By using the *Kirchhoff approximation* [3,14], these currents are obtained directly from the incident wave:

$$\mathbf{J}_a = \hat{n}_a \times \mathbf{H}^i \tag{1.a}$$

$$\mathbf{M}_a = -\hat{n}_a \times \mathbf{E}^i \tag{1.b}$$

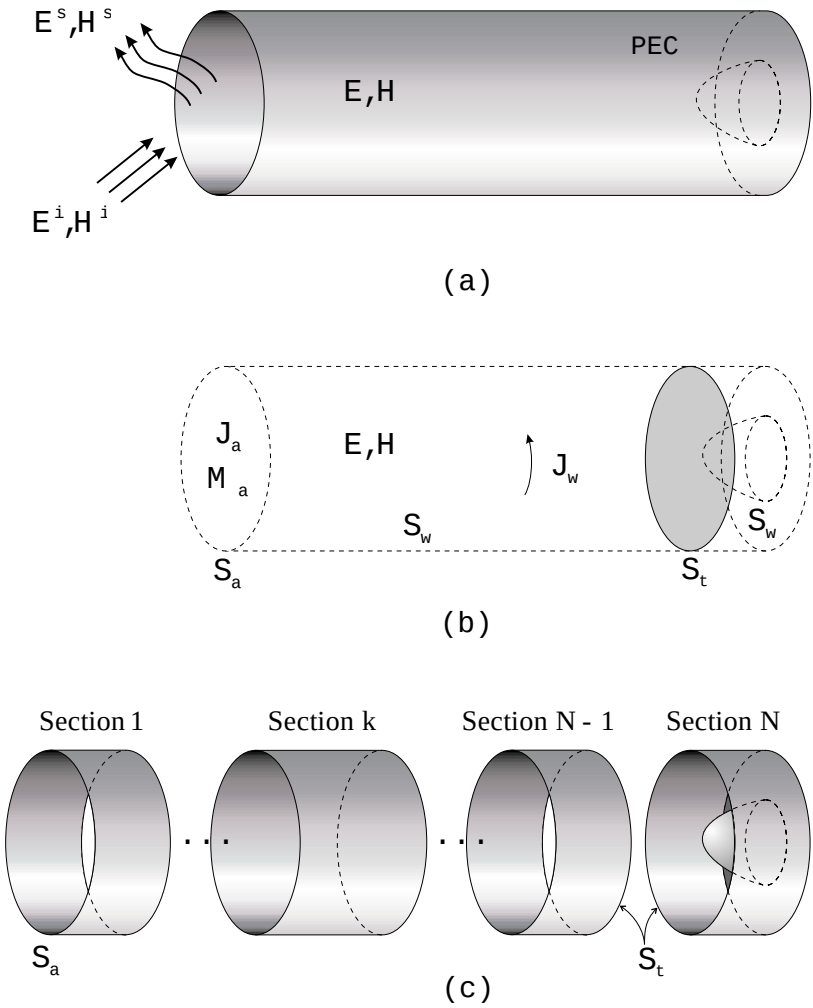

Figure 1. The cavity model. (a) Original problem; (b) Equivalent problem; (c) Segmented problem.

Once the equivalent problem is solved, the external scattered fields are obtained by evaluating a *generalized reciprocity integral* [10–12] over a surface S_t located close to the cavity termination:

$$\mathbf{p} \cdot \mathbf{E}^s(\mathbf{r}) \approx \int_{S_t} (\mathbf{E}_t^- \times \mathbf{H}_t^+ - \mathbf{E}_t^+ \times \mathbf{H}_t^-) \cdot \hat{n}_t \; ds \tag{2}$$

where $\mathbf{E}^s$ is the scattered field at the observation point $\mathbf{r}$, $\mathbf{p}$ is the

strength of an electric current point (test) source also located in $\mathbf{r}$, $\{\mathbf{E}_t^-, \mathbf{H}_t^-\}$ are the fields scattered by the termination in the cavity, while $\{\mathbf{E}_t^+, \mathbf{H}_t^+\}$ are the fields radiated by the test source in the presence of the cavity structure without the termination. The application of the RI involves two advantages. First, the fields coupled into the cavity only need to be tracked one-way down the duct to the surface S_t, and not back. On the other hand, the analysis of the entire cavity can be separated into two independent parts: one deals with the cavity duct alone and the other with the termination. So, the termination, which usually contains complex obstacles, can be analyzed by using more rigorous numerical methods [11–13].

Another possibility is the *aperture integration* technique in which *Kirchhoff approximation* is used again and the outgoing fields in the aperture $\{\mathbf{E}_a^-, \mathbf{H}_a^-\}$ are integrated over S_a to obtain the external scattered fields. This technique has been used in most works about cavities although we have chosen the RI because of the previously commented advantages.

2.3 Segmentation Algorithm

Let us consider the network model shown in Fig. 1c where the cavity is divided into N sections. The last section contains the complex termination, and whose aperture corresponds with S_t.

First, an appropriate model for the front section of the cavity – Fig. 2a – has to be found. The tangential components of the fields $\{\mathbf{E}_a,\ \mathbf{H}_a\}$ over S_a must be related with the fields $\{\mathbf{E}_t,\ \mathbf{H}_t\}$ over S_t.

These fields can be broken down into a sum of a $(+\hat{z})$ travelling and a $(-\hat{z})$ travelling components in each extreme of the duct as follows:

$$\mathbf{E}_a = \mathbf{E}_a^+ + \mathbf{E}_a^- \tag{3.a}$$

$$\mathbf{H}_a = \mathbf{H}_a^+ + \mathbf{H}_a^- \tag{3.b}$$

$$\mathbf{E}_t = \mathbf{E}_t^+ + \mathbf{E}_t^- \tag{3.c}$$

$$\mathbf{H}_t = \mathbf{H}_t^+ + \mathbf{H}_t^- \tag{3.d}$$

where superindex $(+)$ notes propagation in $(+\hat{z})$ direction, while $(-)$ notes propagation in $(-\hat{z})$ direction.

For our convenience, let us define the vectors:

$$\underline{W}_a^+ = \begin{pmatrix} \mathbf{E}_a^+ \\ \mathbf{H}_a^+ \end{pmatrix} \tag{4.a}$$

$$\underline{W}_a^- = \begin{pmatrix} \mathbf{E}_a^- \\ \mathbf{H}_a^- \end{pmatrix} \tag{4.b}$$

$$\underline{W}_t^+ = \begin{pmatrix} \mathbf{E}_t^+ \\ \mathbf{H}_t^+ \end{pmatrix} \tag{4.c}$$

$$\underline{W}_t^- = \begin{pmatrix} \mathbf{E}_t^- \\ \mathbf{H}_t^- \end{pmatrix} \tag{4.d}$$

containing both electric and magnetic tangential components over surfaces S_a and S_t.

Thus, the front section may be characterized by the following matrix equation

$$\begin{pmatrix} \underline{W}_a^- \\ \underline{W}_t^+ \end{pmatrix} = \begin{bmatrix} \underline{\underline{S}}_{11} & \underline{\underline{S}}_{12} \\ \underline{\underline{S}}_{21} & \underline{\underline{S}}_{22} \end{bmatrix} \cdot \begin{pmatrix} \underline{W}_a^+ \\ \underline{W}_t^- \end{pmatrix} = \underline{\underline{S}} \cdot \begin{pmatrix} \underline{W}_a^+ \\ \underline{W}_t^- \end{pmatrix} \tag{5}$$

where $\underline{\underline{S}}$ is a scattering matrix.

This model can be generalized to any of the N subsections in which the cavity is split, see Fig. 2b. Accordingly, the *k-th* subsection will be characterized by:

$$\begin{pmatrix} \underline{W}_k^- \\ \underline{W}_{k+1}^+ \end{pmatrix} = \begin{bmatrix} \underline{\underline{S}}_{11}^{(k)} & \underline{\underline{S}}_{12}^{(k)} \\ \underline{\underline{S}}_{21}^{(k)} & \underline{\underline{S}}_{22}^{(k)} \end{bmatrix} \cdot \begin{pmatrix} \underline{W}_k^+ \\ \underline{W}_{k+1}^- \end{pmatrix} = \underline{\underline{S}}^{(k)} \cdot \begin{pmatrix} \underline{W}_k^+ \\ \underline{W}_{k+1}^- \end{pmatrix} \tag{6}$$

where subindex k and $k+1$ are used to note the tangential components of the fields over surfaces S_k and S_{k+1}.

So, the global scattering matrix of the front section may be obtained by cascading the scattering matrices of the $N-1$ individual subsections. Thus far, we have not done any approximation in the formulation, therefore its accuracy will be only influenced by the own limitations of the numerical method used to determine the scattering matrices $\underline{\underline{S}}^{(k)}$, which will be detailed in the following section. By taking into account the characteristics of the usual cavities into study (geometrically smooth and electrically large), the *Kirchhoff approximation* [14] can be used to ignore any reflections caused by the front section waveguide duct. Which entails considering

$$\underline{\underline{S}}_{11}^{(k)} = \underline{\underline{S}}_{22}^{(k)} = 0 \ \ \forall\, k \tag{7}$$

so equation (6) becomes:

$$\underline{W}_k^- = \underline{\underline{S}}_{12}^{(k)} \cdot \underline{W}_{k+1}^- \tag{8}$$

$$\underline{W}_{k+1}^+ = \underline{\underline{S}}_{21}^{(k)} \cdot \underline{W}_k^+ \tag{9}$$

The coupling of the incident wave from the aperture S_a (or S_1) to the termination S_t (or S_N) is obtained as:

$$\underline{W}_N^+ = \underline{\underline{S}}_{21}^{(N-1)} \cdots \underline{\underline{S}}_{21}^{(1)} \cdot \underline{W}_1^+ \tag{10}$$

taking into account that $\underline{W}_1^+ = \underline{W}_a^+$ and $\underline{W}_N^+ = \underline{W}_t^+$ the last expression may be expressed as

$$\underline{W}_t^+ = \underline{\underline{S}}_{21}^{(N-1)} \cdots \underline{\underline{S}}_{21}^{(1)} \cdot \underline{W}_a^+ \tag{11}$$

where $\underline{W}_a^+$ and $\underline{W}_t^+$ are related throughout the multiplication of the transmission sub-blocks $\underline{\underline{S}}_{21}^{(k)}$ of the generalized scattering matrices $\underline{\underline{S}}^{(k)}$.

This approach is computationally much more efficient than other methods such as [16], where the scattering matrix was obtained by standard *Method of Moments* (MoM). In this previous work, the whole scattering matrix was obtained without doing any simplification, thus it was restricted to very small cavities due to computational and storage requirements.

On the other hand, the final section may be characterized as a one-port load with its proper generalized reflection coefficient $\underline{\underline{\Gamma}}$ (Fig. 2b).

$$\underline{W}_t^- = \underline{\underline{\Gamma}} \cdot \underline{W}_t^+ \tag{12}$$

It must be pointed that equations (11) and (12) allow to obtain both incident and reflected fields ($\underline{W}_t^+$ and $\underline{W}_t^-$) over S_t, due to the excitation $\underline{W}_a^+$ over the cavity mouth S_a. These are the fields involved in the RI expression (2), which must be evaluated to calculate the response of the entire cavity. The fields $\underline{W}_a^+$ are obtained as the tangential components of the incident fields over the aperture S_a, closely related to the equivalent currents $\mathbf{J}_a$ and $\mathbf{M}_a$.

Otherwise, when the AI is used instead of RI, the fields need to be tracked back from the termination S_t to the aperture S_a; this may

be easily done employing the previous model, by simply multiplying the transmission sub-blocks $\underline{\underline{S}}_{12}^{(k)}$:

$$\underline{W}_a^- = \underline{\underline{S}}_{12}^{(1)} \cdot \cdots \cdot \underline{\underline{S}}_{12}^{(N-1)} \cdot \underline{W}_t^- \tag{13}$$

Nevertheless, this approach duplicates the computational cost with respect to RI, so in the rest of the paper will be only concerned with the RI solution.

2.4 Scattering Matrices

The generalized scattering matrix of each section – Fig. 2(b) – can be calculated by using any method that allows a good grade of accuracy with moderate computational complexity. Both IPO and PPO methods have been shown to be two efficient HF alternatives for analyzing shallow and moderately large cavities. So that they are suitable to be implemented for the smooth duct sections where the *Kirchhoff approximation* (and consequently the segmented algorithm) is applicable. The formulation of both IPO and PPO methods is common in the task of calculating the $\underline{\underline{S}}_{21}^{(k)}$ transmission sub-blocks, that are obtained by solving the *magnetic field integral equation* (MFIE) for the equivalent currents in the interior section walls:

$$\begin{aligned}\mathbf{J}_{w,k}(\mathbf{r}) = {} & 2 \cdot \hat{n}_{w,k} \times \mathbf{H}_k^{inc}(\mathbf{r}) \\ & + 2 \cdot \hat{n}_{w,k} \times PV \int_{S_{w,k}} \mathbf{J}_{w,k}(\mathbf{r}') \times \nabla G_0(\mathbf{r}-\mathbf{r}')\, ds'\end{aligned} \tag{14}$$

where $\mathbf{H}_k^{inc}(\mathbf{r})$ is the incident field over the *k-th* section walls $S_{w,k}$, which is calculated using the *Kirchhoff approximation* as:

$$\begin{aligned}\mathbf{H}_k^{inc}(\mathbf{r}) = {} & \int_{S_k} \hat{n}_k \times \mathbf{H}_k^+(\mathbf{r}') \times \nabla G_o(\mathbf{r}-\mathbf{r}')\, ds' \\ & + \frac{1}{jk\eta_o} \nabla \times \int_{S_k} \mathbf{E}_k^+(\mathbf{r}') \times \hat{n}_k \times \nabla G_o(\mathbf{r}-\mathbf{r}')\, ds'\end{aligned} \tag{15}$$

The symbol $PV\int$ stands for the principal value of the integral and ∇G_0 is the gradient of the free space Green's function given by

$$\nabla G_0(\bar{R}) = \hat{R}\left(jk + \frac{1}{R}\right)\frac{e^{-jkR}}{4\pi R} \tag{16}$$

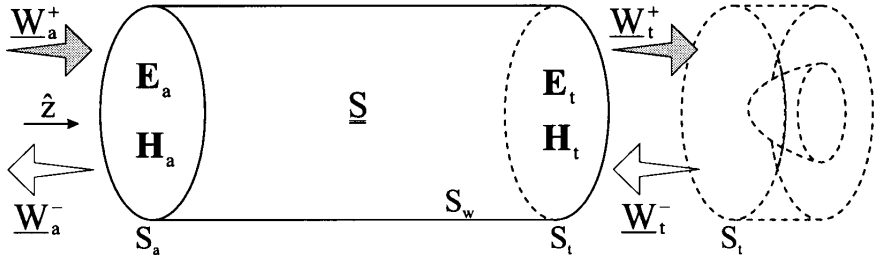

(a) Front part

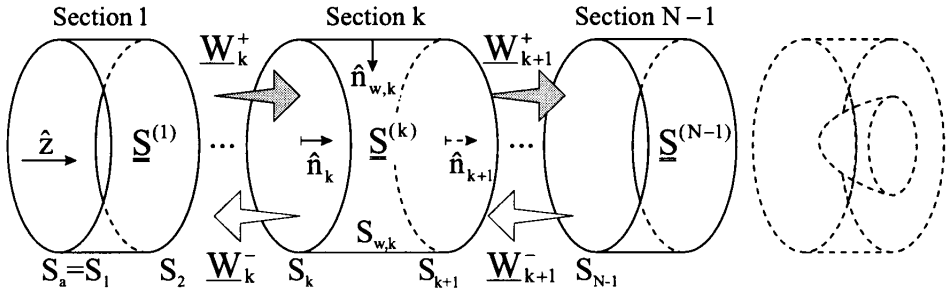

(b) Front part split into several sections

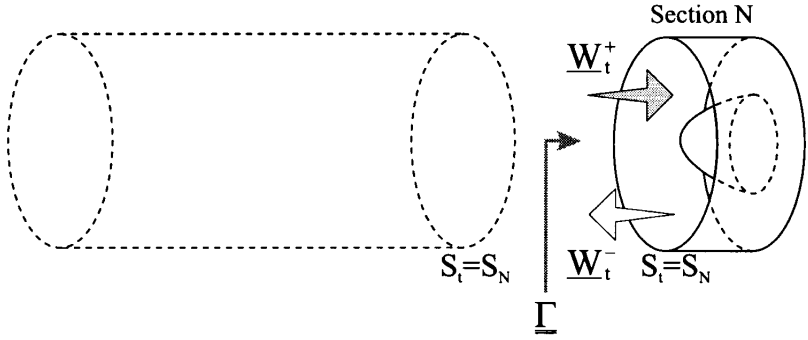

(c) Termination section

Figure 2. Cavity geometry.

where $R = |\bar{R}|$ and $\hat{R} = \bar{R}/R$

Equations (14) and (15) are implemented for each section by modeling its aperture, walls and termination with flat facets [7–9]. The integrals are evaluated numerically via summations by assuming the fields and currents are constant over each facet. These currents are found via an iterative process, which may be IPO or PPO.

The practical approach for the PPO method [8, 9] is based on taking into account that smooth sections are being considered, in which it could be expected that most of the energy flows towards the end of the section and not in the backwards direction. The PPO implementation of (14) consists of integrating the currents progressively, according to the propagation process inside a smooth waveguide, so each facet radiates only over those facets that are closer to the termination. This process is equivalent in such a way to analyze each facet considering a variable number of iterations, which becomes higher as the facets are closer to the termination.

On the other hand, the IPO method [7, 9] does not take into consideration the one-way propagation of energy so it will be valid for more arbitrary structures. The IPO method solves the MFIE in a number of iterations related to the number of expected internal reflections of importance, in this case one iteration entails the full radiation of each facet over the rest of the facets in the section wall. By using IPO solution for complex geometries, shadowing effects can be included into the integrations, improving greatly the convergence.

Once the wall currents $\mathbf{J}_{w,k}$ are known, the outgoing tangential fields ($\mathbf{E}^{+}_{k+1}$ and $\mathbf{H}^{+}_{k+1}$) over the section end (S_{k+1}), are obtained by integrating $\mathbf{J}_{w,k}$ over the section walls $S_{w,k}$

$$\mathbf{E}^{+}_{k+1}(\mathbf{r}) = \hat{n}_{k+1} \times \left(\frac{\eta_0}{jk} \nabla \times \int\limits_{S_{w,k}} \mathbf{J}_{w,k}(\mathbf{r}') \times \nabla G_0(\mathbf{r} - \mathbf{r}')\, ds' \right) \times \hat{n}_{k+1} \tag{17}$$

$$\mathbf{H}^{+}_{k+1}(\mathbf{r}) = \hat{n}_{k+1} \times \left(\int\limits_{S_{w,k}} \mathbf{J}_{w,k}(\mathbf{r}') \times \nabla G_0(\mathbf{r} - \mathbf{r}')\, ds' \right) \times \hat{n}_{k+1} \tag{18}$$

With respect to the final section (containing the cavity termination), its analysis must be usually carried out via more accurate methods

than the rest of the structure, in order to model properly the special characteristics of this typically complex part of the cavity [11–13].

3. COMPUTATIONAL ASPECTS

One of the most interesting aspects of this segmented technique is the considerable reduction of the computational cost in with respect to the previous methods (IPO and PPO), together with the accuracy of the obtained results.

To account for the computational cost, it is useful to define an *elemental operation* as the radiation from one facet to another – remember that integrals in (14), (15), (17) and (18) are implemented by modeling the surfaces by flat facets –. Table 1 shows the computational complexity of the two approaches, comparing their results when the front section is in a whole piece and when it is split into N subsections. In this table, I and M represent the number of iterations and facets needed to analyze the whole front section; while i and m are the same matters but related to one sub-section. All the subsections are assumed to be equal, so i and m are considered to be the same in all of them. In order to be able to compare the computational costs, we can further take $i \approx I/N$ and $m \approx M/N$ which happens certainly in most practical cases. It can be seen that the segmented versions provide a great reduction in the computational cost with respect the one-section case (a reduction of N^2 for the S-IPO and N for the S-PPO). It must be noticed that the computational cost of the S-PPO is lower than the one of the S-IPO because of the number of iterations required to analyze an individual section will be always greater or equal than unity ($i \geq 1$).

Further advantage is obtained when the cavity is split into equal sections, in this case only one of them must be analyzed, thus the computational cost is reduced by a factor of N^3 for the S-IPO and N^2 for the S-PPO.

	One section	N **sections**
S-IPO	$I \cdot M^2$	$N \cdot i \cdot m^2 \approx I \cdot M^2/N^2$
S-IPO	$M^2/2$	$N \cdot m^2/2 \approx M^2/2N$

Table 1. Computational complexity of both approaches.

4. RESULTS

The method described above has been applied to several examples in order to demonstrate its efficiency and accuracy. The results are monostatic copolarized RCS which is plotted as a function of aspect angle for planewave incidence. The RCS (σ) is given by

$$\sigma = \lim_{r\to\infty} 4\pi r^2 \frac{|\bar{E}^s(\bar{r})|^2}{|\bar{E}^i|^2} \tag{19}$$

where $E^s(\bar{r})$ is the scattered field obtained by using the RI (2) over S_t and $|\bar{E}^i|$ is the magnitude of the incident plane wave. Both $\hat{\theta}$ and $\hat{\phi}$ polarizations are taken into account and compared with a reference solution calculated using modal analysis [1].

A cylindrical cavity of radius $a = 3.5\lambda$ and depth $L = 21\lambda$ is considered with a discretization of 9 $facets\,/\,\lambda^2$. This cavity is split into a variable number of identical sections and the scattering matrices are obtained by using IPO (with an appropriate number of iterations) or PPO. The last section is considered to be only a PEC circular plate (short circuit) which corresponds with the cavity termination; so, the surface S_t is placed just in the cavity end. This kind of termination is used because its generalized reflection coefficient $\underline{\underline{\Gamma}}$ can be easily calculated by invoking the image theory approach [15]. The rest of the sub-sections in which the cavity is split are identical; thus we only need to calculate one scattering matrix in each RCS computation.

Figure 3 shows a comparison between the results generated by the S-IPO with different number of sections and a reference modal solution. The cavity has been analyzed connecting: 1 section (3 iterations were needed), 2 sections (2 iterations) and 3 sections (1 iteration). From this figure we see that the S-IPO method performs very well the RCS pattern in all the cases.

Fig. 4 shows the RCS results obtained by the S-PPO method for the same cavity and with the same number of sections (1, 2 and 3). It can be seen that a good grade of accuracy is also achieved in this case, although worse than that obtained by S-IPO. However, the S-PPO has the advantage that its computational cost is lower, as can be seen in Table 2.

	1 sections	**2 sections**	**3 sections**
S-IPO	100 %	16 %	3.7 %
S-IPO	16 %	4 %	1.8 %

Table 2. Relative computational cost, (%)

It must be noticed that Table 2 was obtained taking into account that the sections are identical, so only one section has been analyzed. It can be seen that the computational cost decreases as the number of sections increases. Nevertheless, there is a limit in the number of sections, because too many sections produce significant numerical errors due to the discretization process involved in the cross section of each junction. It has been found that a section whose depth is similar to the cross section diameter uses to be a good choice.

5. CONCLUSIONS AND DISCUSSION

A segmented approach for both IPO and PPO methods has been described in this paper for analyzing the electromagnetic scattering from electrically large and deep cavities. The response of the whole cavity is obtained by splitting the cavity into sections, analyzing this sections separately and finally connecting them to evaluate a generalized reciprocity integral in a surface close to the termination. This connection algorithm is similar to the one described in [16], where the scattering matrix was obtained by standard *Method of Moments* (MoM). In this previous work, the whole scattering matrix was obtained without doing any simplification, thus the method was restricted to very small cavities due to the high computational cost and storage requirements. Both S-IPO and S-PPO use the *Kirchhoff approximation* and the *generalized reciprocity integral* to greatly simplify the connecting scheme, which allows both methods to be used for very large and deep cavities. Otherwise, both methods are suitable to be implemented in parallel processors which implies additional computational advantages.

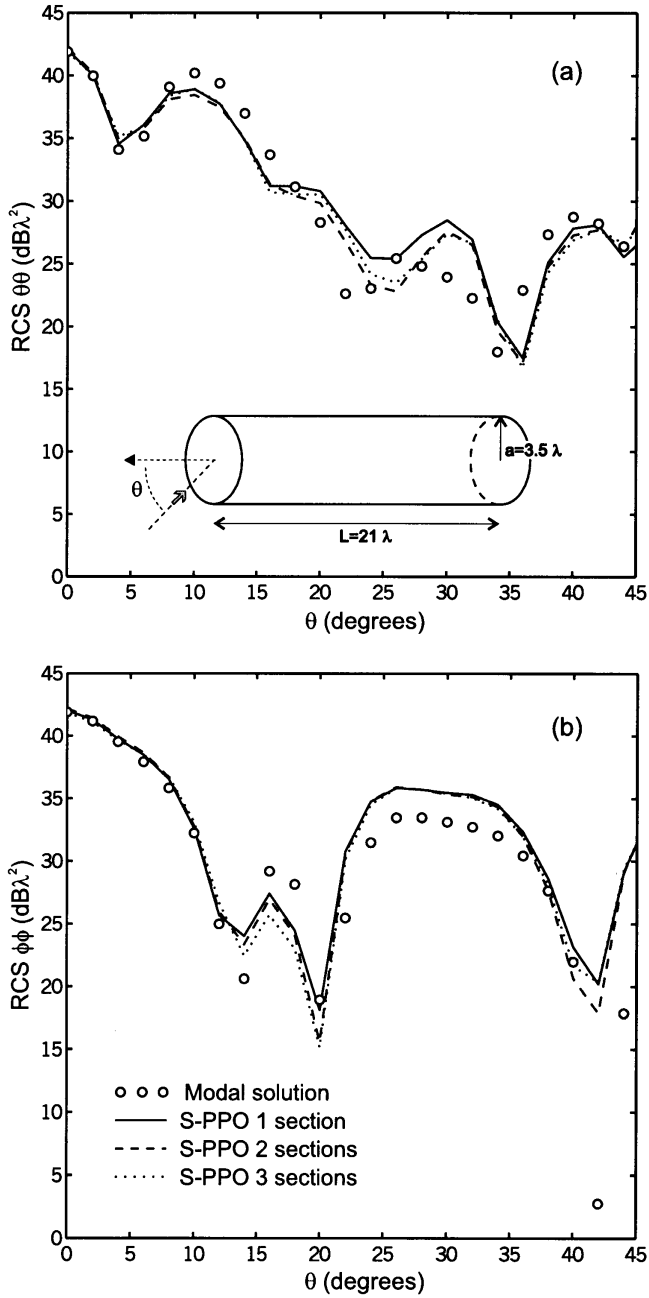

Figure 4. RCS of a cylindrical cavity of radius $a = 3.5\lambda$ and depth $L = 21\lambda$ using S-PPO with a variable number sections.

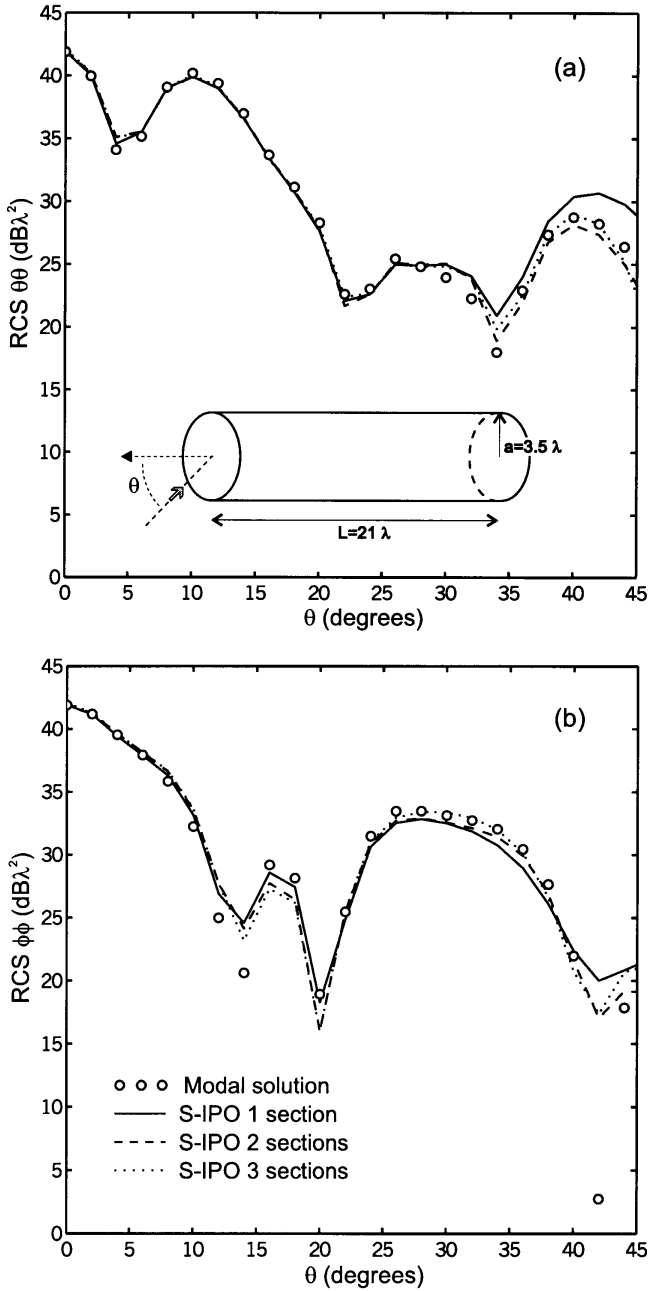

Figure 3. RCS of a cylindrical cavity of radius $a = 3.5\lambda$ and depth $L = 21\lambda$ using S-IPO with a variable number sections.

The computational cost of the S-IPO is reduced by a factor of N^2 (or even N^3 when the sections are identical) with respect to conventional IPO; while in the case of S-PPO it is reduced by a factor of N (or even N^2), where N is the number of sections. It is clear that both methods entail a drastic improvement in the efficiency of the previous methods based on iterative solutions of the MFIE, enhancing its scope of application to deeper cavities. Nevertheless, it must be pointed out that when the number of sections increases, the results become highly dependent on the accuracy obtained in the transmission matrix calculations; so in these cases the S-IPO is preferable than the S-PPO because it provides more accurate results, although it needs more computational cost.

REFERENCES

1. Lee, C. S., and S. W. Lee, "RCS of a coated circular waveguide terminated by perfect conductor," *IEEE Transactions on Antennas and Propagation,* Vol. AP–43, No. 4, 391–398, April 1987.
2. Alintas, A., P. H. Pathak, and M. C. Liang, "A selective modal scheme for the analysis of EM coupling into or radiation from large open-ended waveguides," *IEEE Transactions on Antennas and Propagation,* Vol. AP–36, No. 1, 84–96, January 1988.
3. Pathak, P. H., and R. J. Burkholder, "Modal ray and beam techniques for analyzing the EM scattering by open-ended waveguide cavities," *IEEE Transactions on Antennas and Propagation,* Vol. 37, No. 5, 635–647, May 1989.
4. Ling, H., R. C. Chou, and S. W. Lee, "Shooting and bouncing rays: calculating the RCS of an arbitrary shaped cavity," *IEEE Transactions on Antennas and Propagation,* Vol. 37, No. 2, 194–205, February 1989.
5. Burkholder, R. J., R. C. Chou, and S. W. Lee, "Two-ray shooting methods for computing the EM scattering by large open-ended cavities," *IEEE Computer Physics Communication,* Vol. 68, No. 1–3, 353–365, November 1991.
6. Pino, A. G., F. Obelleiro, and J. L. Rodriguez, "Scattering from conducting open cavities by generalized ray expansion," *IEEE Transactions on Antennas and Propagation,* Vol. AP–41, No. 7, 989–992, July 1993.
7. Obelleiro, F., J. L. Rodriguez, and R. J. Burkholder, "An iterative physical optics approach for analyzing the electromagnetic scattering by large open-ended cavities," *IEEE Transactions on Antennas and Propagation,* Vol. 43, No. 4, 356–361, April 1995.

8. Obelleiro, F., J. L. Rodriguez, and A. G. Pino, "A progressive physical optics (PPO) method for computing the electromagnetic scattering of large open-ended cavities," *Microwave and Optical Technology Letters ,* Vol. 14, No. 3, 166–169, February 1997.
9. Rodriguez, J. L., F. Obelleiro, and A. G. Pino, "Iterative solutions of MFIE for computing electromagnetic scattering of large open-ended cavities," *IEE Proceedings Microwave Antennas Propagation,* Vol. 144, No. 2, 141–144, April 1997
10. Pathak, P. H., and R. J. Burkholder, "A reciprocity formulation for the EM scattering by an obstacle within a large open cavity," *IEEE Transactions on Microwave Theory and Techniques,* Vol. 41, No. 4, 702–707, April 1993.
11. Rousseau, P. R., and R. J. Burkholder, "A hybrid approach for calculating the scattering from obstacles within large, open cavities," *IEEE Transactions on Antennas and Propagation,* Vol. 43, No. 10, 1068–1075, October 1995.
12. Chia, T. T., and R. J. Burkholder, "The application of FDTD in hybrid methods for cavity scattering analysis," *IEEE Transactions on Antennas and Propagation,* Vol. 43, No. 10, 1082–1090, October 1995.
13. Ross, D. C., J. L. Volakis, and H. T. Anastassiu, "Hybrid finite element-modal analysis of jet engine inlet scattering," *IEEE Transactions on Antennas and Propagation,* Vol. 43, No. 3, 277–285, 1995.
14. Ling, H., and H. Kim, "On the Kirchhoff's approximation to scattering from discontinuities in large waveguide ducts," *Microwave and Optical Technology Letters,* Vol. 7, No. 4, 168–172, 1994.
15. Balanis, C. A., *Advanced Engineering Electromagnetics,* John Wiley & Sons, New York, 1989.
16. Wang, T., and H. Ling, "Electromagnetic scattering from three-dimensional cavities via a connection scheme," *IEEE Transactions on Antennas and Propagation,* Vol. 39, No. 10, 1505–1513, October 1991.